Stem Cell Reports
Report
OPEN ACCESS

Human Teratoma-Derived Hematopoiesis Is a Highly Polyclonal Process Supported by Human Umbilical Vein Endothelial Cells

Friederike Philipp,[1,2,4] Anton Selich,[1] Michael Rothe,[1,4] Dirk Hoffmann,[1,4] Susanne Rittinghausen,[2,4,6] Michael A. Morgan,[1,4] Denise Klatt,[1,4] Silke Glage,[3,4] Stefan Lienenklaus,[3] Vanessa Neuhaus,[2,4,6] Katherina Sewald,[2,4,6] Armin Braun,[2,4,6] and Axel Schambach[1,4,5,*]

[1]Institute of Experimental Hematology, Hannover Medical School, Carl-Neuberg-Straße1, 30625 Hannover, Germany
[2]Fraunhofer Institute for Toxicology and Experimental Medicine, 30625 Hannover, Germany
[3]Institute for Laboratory Animal Science, Hannover Medical School, 30625 Hannover, Germany
[4]REBIRTH Cluster of Excellence, Hannover Medical School, 30625 Hannover, Germany
[5]Division of Hematology/Oncology, Boston Children's Hospital, Harvard Medical School, Boston, MA 02115, USA
[6]German Centre for Lung Research DZL, Hannover, Germany
*Correspondence: schambach.axel@mh-hannover.de
https://doi.org/10.1016/j.stemcr.2018.09.010

SUMMARY

Hematopoietic stem cells (HSCs) ensure a life-long regeneration of the blood system and are therefore an important source for transplantation and gene therapy. The teratoma environment supports the complex development of functional HSCs from human pluripotent stem cells, which is difficult to recapitulate in culture. This model mimics various aspects of early hematopoiesis, but is restricted by the low spontaneous hematopoiesis rate. In this study, a feasible protocol for robust hematopoiesis has been elaborated. We achieved a significant increase of the teratoma-derived hematopoietic population when teratomas were generated in the NSGS mouse, which provides human cytokines, together with co-injection of human umbilical vein endothelial cells. Since little is known about hematopoiesis in teratomas, we addressed localization and clonality of the hematopoietic lineage. Our results indicate that early human hematopoiesis is closely reflected in teratoma formation, and thus highlight the value of this model.

INTRODUCTION

Tissue stem cells are the life-long source of organ regeneration. Unlike the origin of solid tissue, development of the hematopoietic stem cells (HSCs) proceeds through distinct stages during embryogenesis (Godin and Cumano, 2002; Mikkola, 2006). The definitive HSCs in vertebrates emerge during a process called endothelial-to-hematopoietic transition (EHT), from hemogenic endothelium (Bertrand et al., 2010; Kissa and Herbomel, 2010). Due to their long-term self-renewal capacities, HSCs are valuable for gene and cell therapies (Morgan et al., 2017). Although many aspects of HSC biology have been elucidated, it remains difficult to generate, maintain, or expand human HSCs. The possibility for *de novo* generation from human induced pluripotent stem cells (hiPSCs) would especially help to relieve the limitation of donor material.

Most differentiation protocols for modeling hematopoiesis are based on small molecules, cytokine supplementation, and timed expression of transcription factors (TFs), following general lines of developmental steps from PSCs to hematopoietic progenitors (Sugimura et al., 2017; Vo and Daley, 2015). These important models, however, fail to mimic the complexity of the cellular environment necessary to support HSC development. The teratoma formation assay offers a three-dimensional (3D) embryonic microenvironment with corresponding tissue patterning, epigenetic imprinting, and extracellular matrices (Damjanov and Andrews, 2016; Gertow et al., 2004). In this surrounding, a low level of spontaneous hematopoiesis occurs and gives rise to engraftable hematopoietic progenitors (Amabile et al., 2013; Suzuki et al., 2013). Implanted osmotic pumps delivering cytokines, such as thrombopoietin and stem cell factor (SCF), can increase the level of hematopoiesis in teratomas (Suzuki et al., 2013). Other protocols use co-injection of murine bone marrow stromal cells (OP9) together with hiPSCs. Further improvement was achieved by the co-injection of genetically modified OP9 expressing Notch ligand Delta-like 1 (Dll1) or Wnt3a (Amabile et al., 2013; Suzuki et al., 2013). Alternatively, murine iPSCs, equipped with an inducible TF (Gfi1b), led to elevated hematopoietic levels after administration of doxycycline (Tsukada et al., 2017). To overcome technical hurdles such as implantation of osmotic pumps, we developed a feasible and less demanding teratoma assay as a robust model for hematopoiesis.

Currently little is known about the origin or maintenance of human hematopoietic cells in teratomas. H&E staining identified hematopoietic cell phenotype in bone marrow-like structures in teratomas (Amabile et al., 2013). Others showed putative hematopoietic cells to reside in close proximity to liver cells, mesenchymal stroma, or yolk sac structures (Damjanov and Andrews, 2016). In a murine iPSC teratoma system, there is evidence that hematopoiesis occurs by EHT (Tsukada et al., 2017). Using our optimized system for human hematopoiesis, we extensively evaluated

the origin and cellular environment of human hematopoietic cells in teratomas via detailed multicolor fluorescent immunohistochemistry (IHC).

To use teratomas to investigate processes of human embryogenesis or hematopoiesis, improved characterization of clonal development is necessary. Blum and Benvenisty (2007) addressed this by mixing three human embryonic stem cell (hESC) lines for teratoma induction. Microsatellite signatures in microdissections of teratoma structures revealed a mixed composition of hESC lines, indicating a polyclonal origin. This important finding illustrates the high impact of environmental cues on differentiation rather than clonal preferences. In our study, we used lentiviral genetic barcode labeling to monitor several thousand clones throughout teratoma development with specific emphasis on hematopoiesis.

In summary, this study provides detailed analysis of hematopoietic teratoma cell localization and clonal development as well as a feasible protocol to generate elevated hematopoiesis levels.

RESULTS

Low Rate of Hematopoiesis in Subcutaneous Teratomas in NSG Mice

To test the level of spontaneous hematopoiesis in teratomas, we injected 1–5 × 10^6 CD34-derived hiPSCs (CD34hiPSC16) subcutaneously into the flanks of NSG mice. Teratomas were isolated once they reached a diameter of about 1.5 cm, which took 45 ± 8 days (mean ± SD). Quantification of hematopoietic cells was accomplished by flow cytometry (FC). To exclude false-positive results due to antibody cross-reactions with damaged cells, we applied a gating strategy that relied upon viability staining and isotype controls (Figure S1A). Overall, teratomas (n = 3) displayed a low spontaneous rate of hematopoietic differentiation (Figure 1A). IHC staining of teratoma sections for the specific markers confirmed low abundance of $CD45^+$ cells (Figure 1B). Of note, CD34 expression occurred in cell clusters whereas the rare $CD45^+$ hematopoietic cells were found distributed throughout the tissue (Figure 1B).

Co-injection of HUVECs Supports Hematopoiesis in Teratomas

Due to the low rate of $CD45^+$ cells in NSG mice and to better mimic a suitable environment for hematopoiesis in the teratoma, we co-injected either human umbilical vein endothelial cells (HUVECs) or murine stromal cell line OP9 together with hiPSCs. The latter are known to elevate hematopoietic output in teratomas (Amabile et al., 2013; Chen et al., 2015; Suzuki et al., 2013). HUVECs were selected because of their instructive signals for the development of hematopoietic cells from vascular endothelium *in vitro* (Gori et al., 2015; Lis et al., 2017). We applied 5 × 10^6 hiPSCs and 1 × 10^6 of the respective supporter cell type for these co-injection experiments. Co-transplantation of OP9 (n = 4) generated a human $CD34^-/CD45^+$ population with a median below 0.5% (Figure 1C). Co-injection of HUVECs (n = 6) resulted in a hematopoietic population with a median of 0.7%. In contrast to former teratoma studies (Amabile et al., 2013; Suzuki et al., 2013), our FC analyses detected no migration of hiPSC-derived $CD34^+$ or $CD45^+$ hematopoietic cells in peripheral blood (PB) or bone marrow (BM) of teratoma-bearing mice.

Elevated Levels of Hematopoietic Cells by Systemic Administration of Human Cytokines

Since co-injection experiments did not efficiently increase hematopoiesis, we explored whether cytokine application can be supportive in this setting. Human interleukin-3 (IL-3), granulocyte macrophage-colony stimulating factor (GM-CSF), and SCF foster hematopoietic progenitor maintenance and expansion (Lemoli and Gulati, 1993). Instead of additive cytokine administration we employed NSGS mice, which systemically express all three cytokines in the NSG mouse background. Teratomas induced with hiPSCs alone (n = 6) in NSGS showed a median of 1.2% hematopoietic cells ($CD34^-/CD45^+$) (Figure 1D). These results were reproducible for a human newborn foreskin fibroblast-derived (Nuff-hiPSC) hiPSC clone. The hematopoietic population comprised a median of 0.9% $CD34^-/CD45^+$ cells (n = 2), comparable with teratomas generated with hiPSCs (Figure 1D). Encouraged by these results, we tested whether the contribution of hematopoietic cells could be increased by co-injection of OP9 (n = 4) or HUVECs (n = 5). Indeed, we saw synergistic effects of the supporter cells and cytokine background (Figure 1D). HUVEC co-transplanted teratomas contained a significantly larger hematopoietic population ($CD34^-/CD45^+$) with a median of 6.1% than teratomas generated in NSGS mice with hiPSCs alone (1.2%). Although the level of hematopoietic cells was elevated, no evidence for migration of hiPSC-derived hematopoietic cells was detected in these experiments by FC (PB and BM).

Notch Ligands and WNT3A Overexpressed by HUVECs Do Not Further Promote Hematopoiesis

Although the exact mode of action through which Notch and Wnt3a signaling affect hematopoiesis remain to be fully elucidated, studies do support the importance of both pathways for hematopoiesis (Bigas and Espinosa, 2012; Lento et al., 2013). Most importantly, Dll1 or Wnt3a expressed by OP9 were previously used to improve hematopoietic output in teratoma assays (Amabile et al., 2013; Suzuki et al., 2013). To compare the influence of

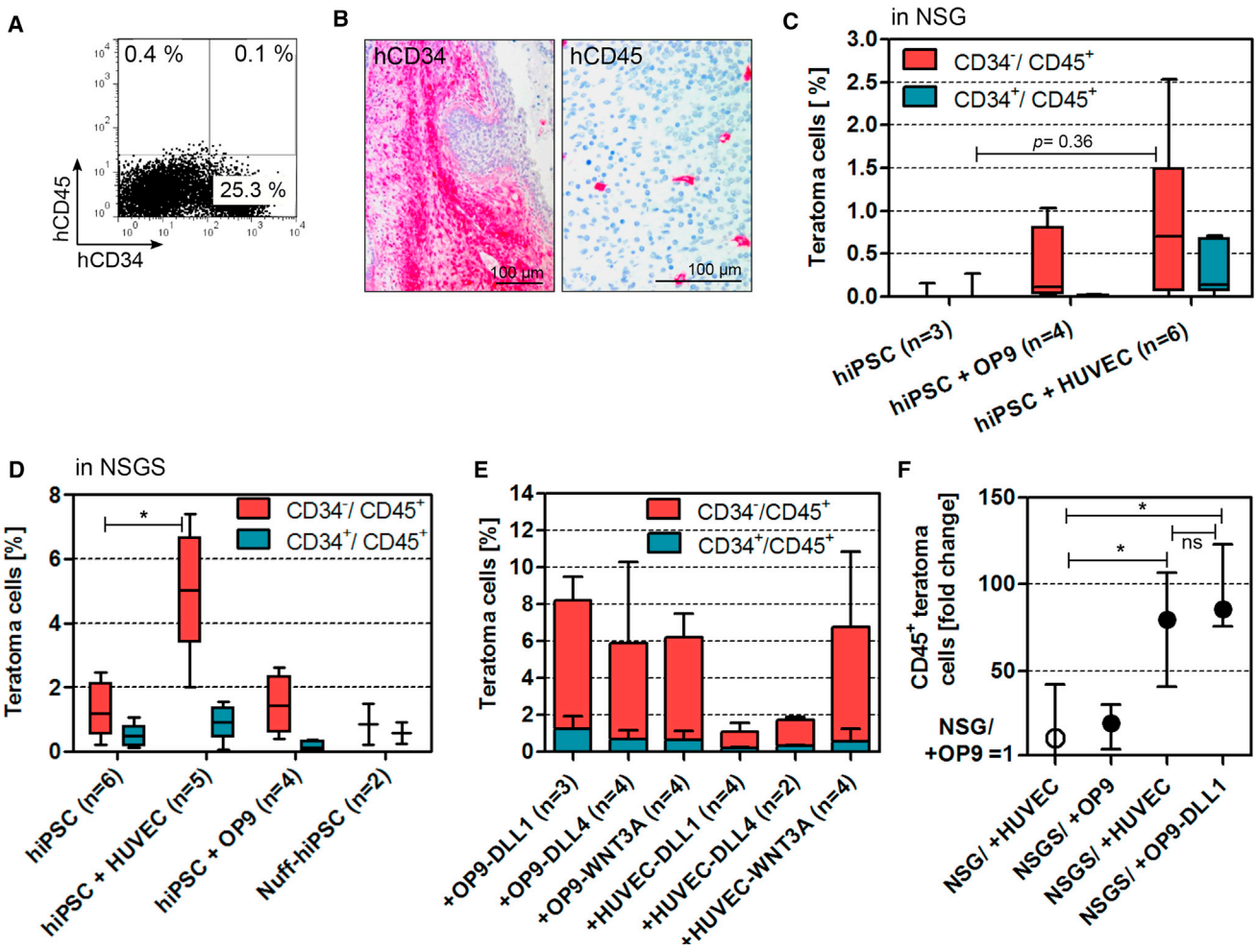

Figure 1. Hematopoiesis in hiPSC-Derived Teratomas Is Improved by Steady Cytokine Supply in NSGS Mice and by Co-injection of HUVECs

(A) Exemplary flow cytometry (FC) detecting hematopoietic marker CD45 and progenitor marker CD34 in a teratoma generated in NSG mice.

(B) Immunohistochemistry on teratomas generated in NSG mice.

(C) FC summary of hematopoietic populations in teratomas generated with or without hematopoietic supporter cells. Median, quartiles, and outer values are depicted.

(D) Summary of FC analyses of teratoma hematopoietic populations generated in NSGS mice that express IL-3, GM-CSF, and SCF (median, quartiles, and outer values).

(E) Summary of FC results of teratoma samples generated with co-injection of OP9 or HUVECs expressing DLL1, DLL4, or WNT3A (mean and SD).

(F) Fold change of all $CD45^+$ cells in teratomas generated with hiPSC and different supporter cell types in NSG or NSGS mice. The median $CD45^+$ population of teratomas generated in NSG with hiPSC + OP9 was set to a value of 1. Graph depicts median and range.

Statistics of (C), (D), and (F) were calculated by Kruskal-Wallis and Dunn's multiple comparisons tests (*$p < 0.05$).

these signaling pathways on hematopoiesis in teratomas, we designed lentiviral vectors to constitutively overexpress WNT3A, DLL1, or DLL4 in HUVECs and OP9 (Figures S1B–S1D). DLL4 was included because it is known to be crucial for arterial specification, representing the starting point for definitive hematopoiesis (Duarte et al., 2004; Park et al., 2018). In fact, teratomas generated with co-transplanted OP9 expressing DLL1 (n = 3), DLL4 (n = 4), or WNT3A (n = 4) yielded higher $CD45^+$ populations than with OP9 alone (Figure 1E). On the other hand, teratomas with co-injected HUVEC-WNT3A resulted in comparable $CD45^+$ populations than with HUVECs alone. Interestingly, HUVEC-DLL1 or -DLL4 did not mediate any hematopoietic support (Figure 1E). In summary, teratomas generated in NSGS mice with co-injection of unmodified HUVECs or OP9-DLL1 resulted in an

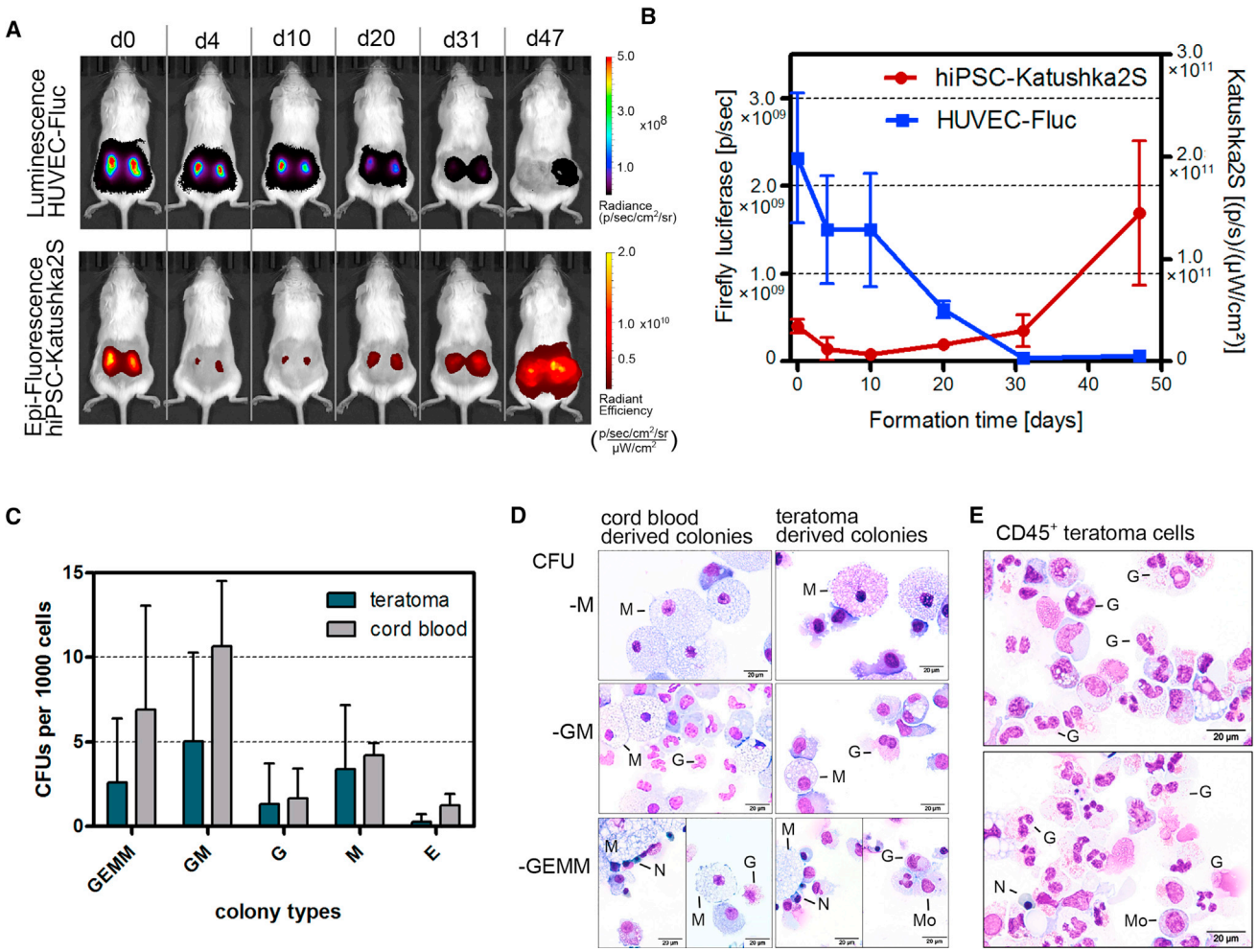

Figure 2. Hematopoiesis in hiPSC-Derived Teratomas Is Improved by Steady Cytokine Supply in NSGS Mice and by Co-injection of HUVECs

(A) Bioluminescent signal of HUVEC-firefly luciferase (Fluc) and red fluorescent signal of hiPSC-Katushka2S (Kat) during teratoma growth in an exemplary NSGS mouse.

(B) Summary of longitudinal study showing bioluminescent signal of HUVEC-Fluc on left y axis and fluorescence signal of hiPSC-Kat on right y axis. Signal intensities were analyzed in regions of interest covering the teratomas at their largest size. Graph displays mean and SD (until day 31 n = 10, day 47 n = 8).

(C) Summary of clonogenic assays for myeloid and erythroid lineages. $CD34^+/CD45^+$ cells were isolated from teratomas (n = 6), generated with hiPSC and HUVECs in NSGS mice. $CD34^+$ cord blood cells were used as control (n = 3). Graph shows mean and SD.

(D) Pappenheim stain of isolated colonies types described in (C).

(E) Pappenheim staining of teratoma-derived $CD45^+$ cells. G, granulocyte; M, macrophage; Mo, monocyte; N, normoblast.

80-fold and 86-fold (medians) greater $CD45^+$ population compared with teratomas generated in NSG mice with co-injected OP9 (Figure 1F).

HUVEC Populations Decline during Teratoma Formation

As HUVECs appeared to promote the hematopoietic population in teratomas, we investigated how long HUVECs are present during teratoma formation. Therefore, we generated HUVECs that expressed firefly luciferase (HUVEC-Fluc) and modified hiPSCs to express the fluorescent protein Katushka2S to monitor teratoma growth (Luker et al., 2015) (Figures S1E and S1F). Within 7 weeks the bioluminescent signal of the co-injected 1×10^6 HUVEC-Fluc decreases to 2.5% of the signal obtained at the day of injection (Figures 2A and 2B). This suggests that the hemogenic support by HUVECs mainly occurred during the first 2–4 weeks.

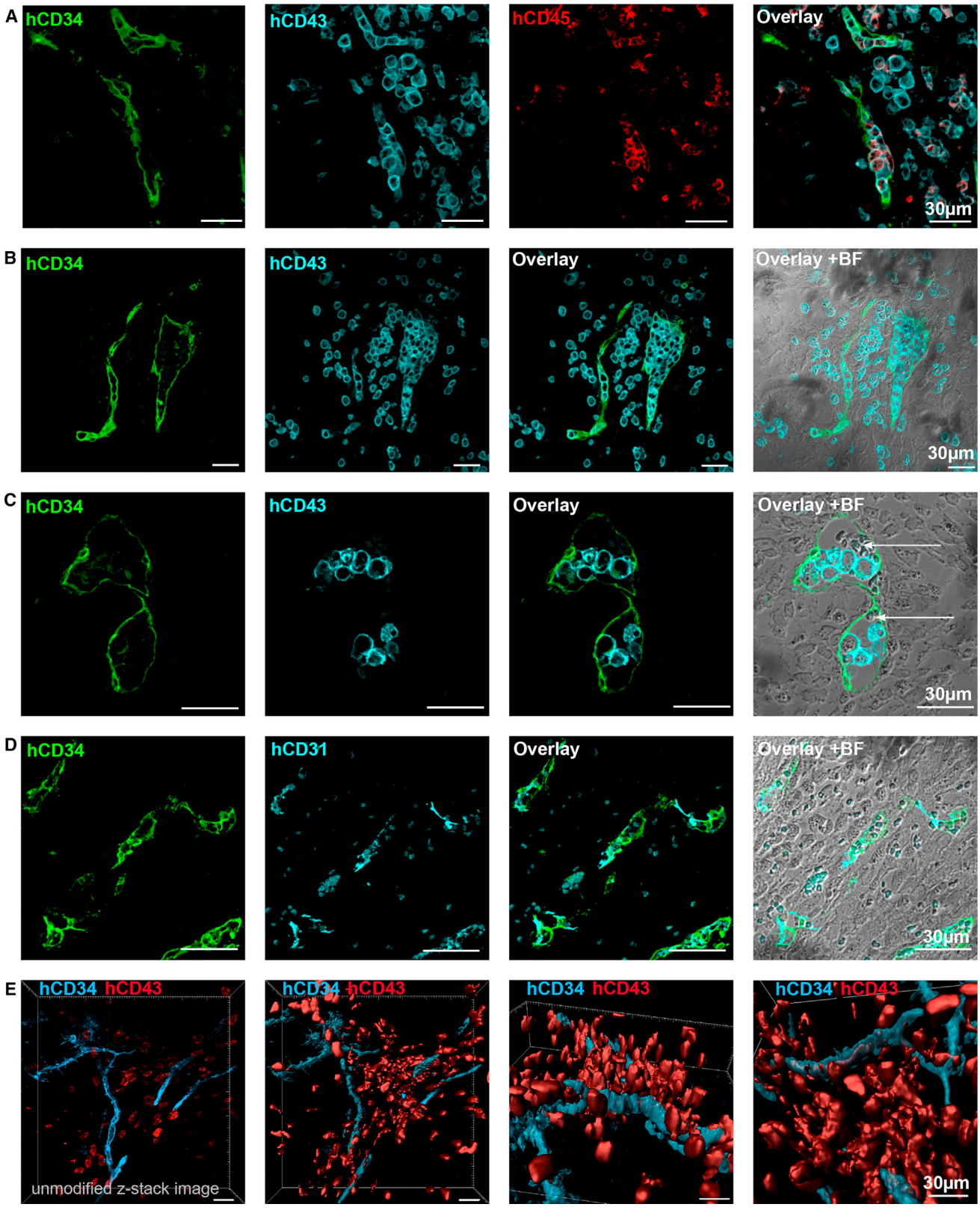

(legend on next page)

We further evaluated lineage capacity of isolated $CD34^+$/$CD45^+$ teratoma cells generated in this setting. Clonogenic assays (n = 6) demonstrated the potential of these cells to produce granulocytes, macrophages, and few immature erythrocytes, which was comparable with freshly isolated $CD34^+$ cord blood cells (n = 3) (Figures 2C and 2D). In Pappenheim staining, cells showed the expected phenotypes of band neutrophils, eosinophils, monocytes, and normoblasts. Sorted $CD45^+$ teratoma populations appeared to consist mainly of monocytes and neutrophils (Figure 2E).

Localization of Hematopoietic Cells inside Vascular Structures

To improve the use of teratoma-linked hematopoiesis as a developmental model, we investigated the points of origin and localization of human hematopoietic cells inside the teratomas. We applied IHC staining on teratoma sections to localize hematopoietic sites in our human setting. All antibodies were validated on appropriate positive and negative controls to ensure specificity for human antigens in this xenograft model. The majority of committed hematopoietic cells ($CD34^-$/$CD43^+$/$CD45^+$) appeared in groups of single cells. Most hematopoietic cells were located close to vascular structures positive for human CD34 (Figures 3A and 3B). Potential events of EHT were implied by co-localization of hematopoietic progenitor cells ($CD34^+$/$CD43^+$/$CD45^+$) surrounded by $CD34^+$ endothelium. In some sections, we identified $CD34^+$ blood vessels with erythrocytes and $hCD43^+$ cells (Figure 3C). To validate the endothelial nature of the $CD34^+$ cells, we also stained sections for the endothelial marker CD31 (Figure 3D). To obtain a more detailed view of the hemogenic vasculature, we recorded z stacks (~100 μm) of stained teratoma slices and calculated 3D models. This approach visualized hematopoietic cell clusters embedded inside and around $CD34^+$ vessels (Figure 3E). Further characterization of the cellular environment of hematopoietic sites showed vascular structures ($CD31^+$) and hematopoietic cells ($CD45^+$) prominently in uniform tissue. Cells appeared to be spindle-shaped or round with scant cytoplasm, which is characteristic for mesenchymal tissue (Figures 3B and 3C, +BF; Figures S2A–S2C). Furthermore, these areas were positive for the mesenchymal intermediate filament vimentin (Figure S2D).

Clonality of Teratoma Formation and Hematopoiesis

Currently it remains to be determined whether teratoma development is subject to clonal pressure or how many hiPSCs of the injected culture contribute to teratoma formation and initiate hematopoiesis. In theory, a teratoma can be generated by a single pluripotent cell. Despite the improvement of hematopoiesis rate, the proportion of hematopoietic progenitors in teratomas remained low in the experiments described above. Therefore, we applied RGB (red, green, blue) labeling combined with nucleotide barcoding (Cornils et al., 2014; Selich et al., 2016) to investigate the frequency of iPSCs, which actually undergo hematopoietic differentiation. This method allowed us to trace clones via genetic labeling. Additional expression of mCherry, Venus, or Cerulean (RGB labeling) also facilitated visual assessment of clonal development (Figure 4A). Transduced hiPSCs were expanded for 21 days (14.6-fold expansion). Additionally, transgene expression was monitored by fluorescence microscopy and FC during the expansion phase and in isolated teratomas, indicating no major transgene silencing *in vitro* or *in vivo* (Figure 4B). Samples were harvested and analyzed after transduction, after *in vitro* expansion, and finally after teratoma formation. The teratoma samples (n = 5) were divided into two sections. One was directly used for sequencing and the second was used to isolate the hematopoietic population by magnetic hCD45 beads followed by sequencing (Figure 4C). Deep sequencing data identified a highly polyclonal composition in hiPSC culture, teratomas, and hematopoietic cells (Figure 4D). Read counts of identical sequences were used as a surrogate marker for clonal contribution of individual barcodes. We observed that only 146 out of 28,300 measured barcodes reoccurred in all $CD45^+$ hematopoietic samples, and 139 out of 21,698 barcodes were detected in all teratoma samples. Hence, thousands of injected cells are capable of forming teratomas and hematopoietic cells (Figures 4E and 4F). In summary, our results suggest that expanded hiPSCs contained a homogeneous pool of cell clones potentially able to form teratomas. Furthermore, several thousand initial hiPSCs revealed the capacity for hematopoietic differentiation.

Figure 3. Human Hematopoietic Cells Localize inside and in Proximity to Vascular Structures of Teratoma

Fluorescent IHC analysis of teratomas generated with hiPSCs in NSGS mice.

(A and B) $CD45^+$/$CD43^+$ cells embedded in $CD34^+$/$CD43^-$/$CD45^-$ vascular tissue (A); $CD43^+$ cells detected inside or in proximity to $CD34^+$ cell clusters (B).

(C) $CD34^+$ vascular structure contained erythrocytes (white arrows) and human hematopoietic cells ($CD43^+$).

(D) Vascularization visualized by staining of CD31 (PECAM-1) and CD34.

(E) z-stack image of a 150-μm stained teratoma slice recorded with a confocal microscope. 3D model was calculated with Imaris software (Bitplane).

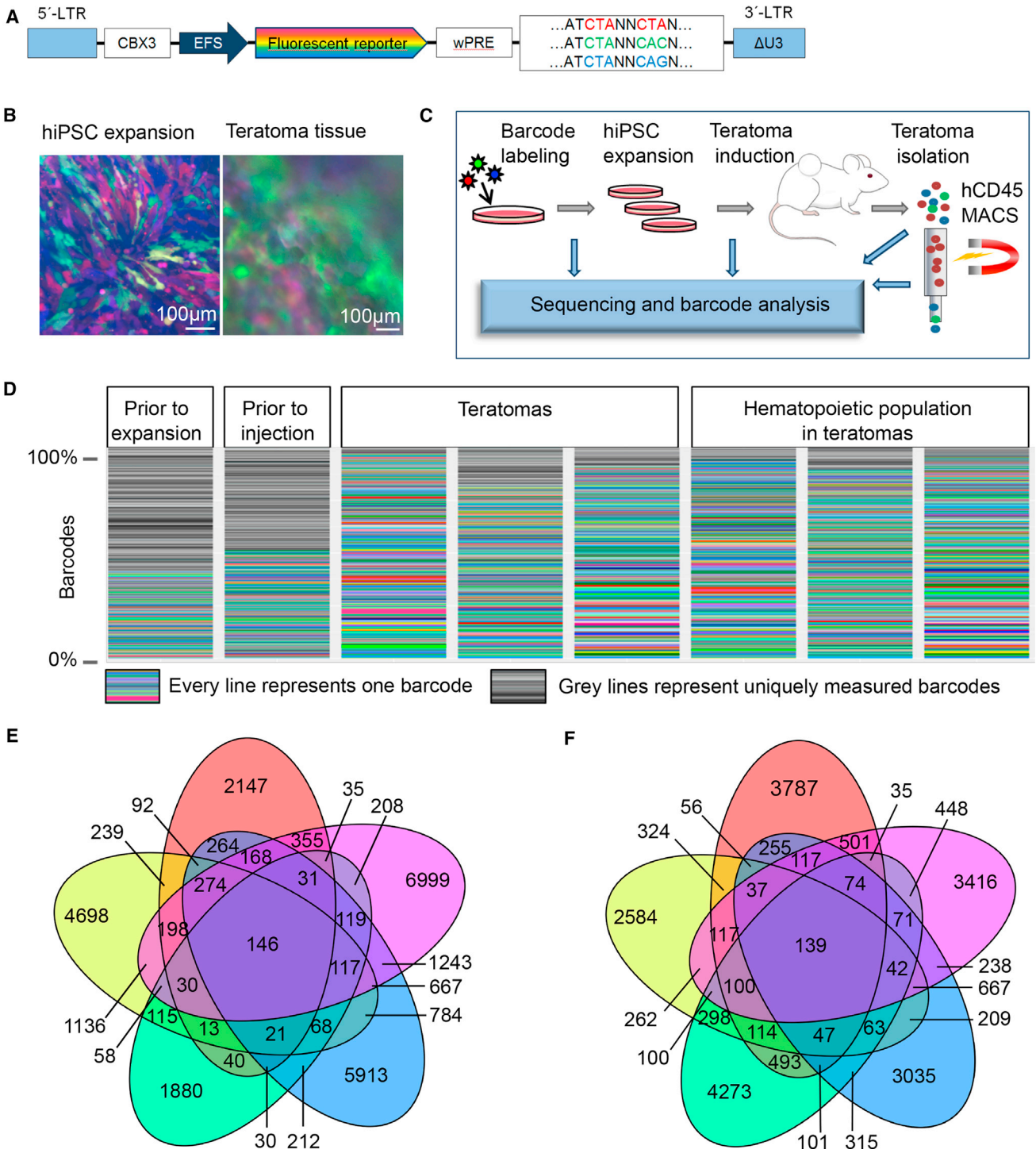

Figure 4. Genetic Barcoding Determined Teratoma Formation and Subsequent Hematopoiesis as Highly Polyclonal Events

(A) Design of the lentiviral construct used to transduce hiPSC prior to teratoma formation. Fluorescent reporters Venus, Cerulean, or mCherry are expressed under an EFS promoter.

(B) Micrographs of fluorescent reporter expression during expansion of hiPSC prior to teratoma induction and after teratoma isolation (38 days).

(legend continued on next page)

DISCUSSION

The teratoma model provides human embryonic tissue to study early hematopoiesis in a physiological 3D environment. However, the $CD45^+$ population in teratomas generated with hiPSCs in NSG mice is low and, thus, hampers its application as a hematopoiesis model. In this study, we elaborated a feasible approach to enhance teratoma-linked hematopoiesis by using NSGS mice. The supply of cytokines by the mouse model is time-saving, easy to perform, and cost-effective. Further enhancement was achieved upon co-injection with supporter cells. HUVECs can promote EHT through vascular induction or support expansion of hematopoietic progenitors from cord blood by secretion of cytokines and growth factors *in vitro* (Lis et al., 2017; Yamaguchi et al., 1996; Yildirim et al., 2005). In the teratoma setting, the presence of HUVECs led to a significant increase in the hematopoietic population in teratomas, although the majority of HUVECs was not maintained beyond 30 days of teratoma formation. Similar levels of hematopoietic cells were obtained with OP9-DLL1, OP9-DLL4, or OP9-WNT3A, but not with OP9 alone. Intriguingly, while co-injection of HUVEC-WNT3A did not further elevate hematopoietic yield compared with HUVECs alone, co-injection of HUVEC-DLL1 or -DLL4 suppressed intra-teratoma hematopoiesis. It remains to be determined whether this was caused by changes in the transcriptome of HUVECs potentially provoked by lentiviral transduction or whether the overexpression of the particular transgenes is not compatible with the support of hematopoiesis by HUVECs.

In summary, the elaborated teratoma formation protocol with HUVECs in NSGS mice provides a decent hematopoietic population and represents a starting point from which to investigate human hematopoiesis with a low technical demand.

The explicit polyclonality of teratoma formation and subsequent hematopoiesis makes this system interesting for additional applications. Future studies could use genetic barcode labeling to mark differentially cultured or transduced hiPSC clones to study their differentiation preferences. Microdissections would allow investigation of potential germ-layer preferences exhibited by different hiPSC clones. In particular, upscaling differentiation protocols could be optimized by selecting the most suitable clone for the specific target lineage. Furthermore, effects of TFs from libraries on teratoma-derived hematopoiesis could be examined closely and might promote valuable insights into developmental states even beyond the hematopoietic system.

Another important asset of the teratoma model is the possibility to localize target cells in tissues assembled in natural structures. In this study, human hematopoietic cell localization was carefully examined by specific detection of surface markers. In rare cases, hematopoietic progenitors were located inside vessels. These results indicate that hiPSC-derived hematopoiesis in teratoma reflects the natural EHT process, which has recently been described for murine teratomas (Tsukada et al., 2017). Further examination of the cellular environment revealed that the majority of hematopoietic and vascular endothelial cells were located in mesenchymal tissue, as identified by cell phenotype and vimentin staining. Whether the hematopoietic cells actively migrate from the vessels into the mesenchyme, or the hemogenic endothelium fully differentiates into $CD34^-/CD45^+$ cells remains unclear. Based on our results, we hypothesize that human hematopoietic cells originate from EHT. The endothelium, in turn, derives from the mesenchymal-to-epithelial transition. Both processes are closely related to normal embryogenesis and affirm the use of the teratoma model to study embryonic processes in healthy and diseased backgrounds.

EXPERIMENTAL PROCEDURES

Mice

All animal experiments were performed in accordance with Lower Saxony State Office for Consumer Protection and Food Safety in Germany. Further details can be found in Supplemental Experimental Procedures.

Teratoma Induction

For injection into mice, hiPSC were harvested using trypsin/EDTA. Unless stated otherwise, cell numbers were adjusted to 3×10^6 hiPSCs per injection. In co-injection experiments, 1×10^6 supporter cells were mixed with hiPSCs prior to injection. Harvested cells were centrifuged at 300 × *g* and gently resuspended in hiPSC medium containing 20 μM Y-27632 (kindly provided by Leibniz University, Hannover). Cell suspensions were cooled to 4°C prior to addition of 100 μL of Matrigel basement membrane matrix (Corning) (Prokhorova et al., 2009). The injection solution was kept at 4°C until subcutaneous injection into the flank. We induced two teratomas per mouse. The injection volume was 150–200 μL. Mice were sacrificed as soon as one teratoma reached 1.5 cm in diameter. After isolation, teratoma tissue was randomly divided into two parts. One was used for IHC and the other for FC.

(C) Experimental scheme to access clonality of teratomas and teratoma-derived hematopoiesis.
(D) Barcode variety in hiPSC cultures and teratoma samples.
(E) Venn diagram depicting barcodes detected in $CD45^+$ samples isolated from teratoma.
(F) Venn diagram depicting barcodes detected in teratoma samples.

Single-Cell Preparation from Teratoma Tissue

Teratomas were sliced into 3- to 5-mm pieces and incubated in DMEM containing 160 U/mL dispase I (Roche) and 2 U/mL collagenase IV (Thermo Fisher Scientific) for 40–60 min at 37°C. Thereafter, suspensions were processed through 70-μm cell strainers (Fisher Scientific). After centrifugation (300 × *g*, 10 min, 4°C), cells were resuspended and incubated with 15–20 μg of DNAse I (STEMCELL Technologies) and kept at room temperature for 15 min. Afterward, cells were washed and used for further experiments.

Statistics

Kruskal-Wallis and Dunn's multiple comparison tests were performed with GraphPad Prism 7 software. Asterisks indicate a p value of less than 0.05.

Further methods are detailed in Supplemental Experimental Procedures.

SUPPLEMENTAL INFORMATION

Supplemental Information includes Supplemental Experimental Procedures and two figures and can be found with this article online at https://doi.org/10.1016/j.stemcr.2018.09.010.

AUTHOR CONTRIBUTIONS

F.P. designed and performed experiments and wrote the manuscript. A. Selich provided barcode technology and analysis. D.H. and D.K. cloned lentiviral constructs. M.A.M. generated NuffhiPSC clone. A. Schambach designed experiments and contributed to lentiviral vectors. S.G. and S.L. supported teratoma experiments. M.R., D.H., V.N., K.S., S.R., M.A.M., A.B., and A. Schambach provided conceptual advice, edited the manuscript, and discussed results.

ACKNOWLEDGMENTS

We thank Gina Geide, Margarethe Schleiss, and Karin Serwatzki for assistance in IHC, and Matthias Meyer and Larissa Buch for support in teratoma experiments. We also thank Mania Ackermann for providing CD34iPSC16 and Bettina Weigel for CB isolation. This work was supported by grants from DFG (REBIRTH Cluster of Excellence and SFB738).

Received: February 23, 2018
Revised: September 19, 2018
Accepted: September 20, 2018
Published: October 18, 2018

REFERENCES

Amabile, G., Welner, R.S., Nombela-Arrieta, C., D'Alise, A.M., Di Ruscio, A., Ebralidze, A.K., Kraytsberg, Y., Ye, M., Kocher, O., Neuberg, D.S., et al. (2013). In vivo generation of transplantable human hematopoietic cells from induced pluripotent stem cells. Blood *121*, 1255–1264.

Bertrand, J.Y., Chi, N.C., Santoso, B., Teng, S., Stainier, D.Y.R., and Traver, D. (2010). Haematopoietic stem cells derive directly from aortic endothelium during development. Nature *464*, 108–111.

Bigas, A., and Espinosa, L. (2012). Hematopoietic stem cells: to be or Notch to be. Blood *119*, 3226–3235.

Blum, B., and Benvenisty, N. (2007). Clonal analysis of human embryonic stem cell differentiation into teratomas. Stem Cells *25*, 1924–1930.

Chen, X., Zhao, Q., Li, C., Geng, Y., Huang, K., Zhang, J., Wang, X., Yang, J., Wang, T., Xia, C., et al. (2015). OP9-Lhx2 stromal cells facilitate derivation of hematopoietic progenitors both in vitro and in vivo. Stem Cell Res. *15*, 395–402.

Cornils, K., Thielecke, L., Hüser, S., Forgber, M., Thomaschewski, M., Kleist, N., Hussein, K., Riecken, K., Volz, T., Gerdes, S., et al. (2014). Multiplexing clonality: combining RGB marking and genetic barcoding. Nucleic Acids Res. *42*, e56.

Damjanov, I., and Andrews, P.W. (2016). Teratomas produced from human pluripotent stem cells xenografted into immunodeficient mice—a histopathology atlas. Int. J. Dev. Biol. *60*, 337–419.

Duarte, A., Hirashima, M., Benedito, R., Trindade, A., Diniz, P., Bekman, E., Costa, L., Henrique, D., and Rossant, J. (2004). Dosage-sensitive requirement for mouse Dll4 in artery development. Genes Dev. *18*, 2474–2478.

Gertow, K., Wolbank, S., Rozell, B., Sugars, R., Andäng, M., Parish, C.L., Imreh, M.P., Wendel, M., and Ährlund-Richter, L. (2004). Organized development from human embryonic stem cells after injection into immunodeficient mice. Stem Cells Dev. *13*, 421–435.

Godin, I., and Cumano, A. (2002). The hare and the tortoise: an embryonic haematopoietic race. Nat. Rev. Immunol. *2*, 593–604.

Gori, J.L., Butler, J.M., Chan, Y., Chandrasekaran, D., Poulos, M.G., Ginsberg, M., Nolan, D.J., Elemento, O., Wood, B.L., Adair, J.E., et al. (2015). Vascular niche promotes hematopoietic multipotent progenitor formation from pluripotent stem cells. J. Clin. Invest. *125*, 1–12.

Kissa, K., and Herbomel, P. (2010). Blood stem cells emerge from aortic endothelium by a novel type of cell transition. Nature *464*, 112–115.

Lemoli, R.M., and Gulati, S.C. (1993). Effect of stem cell factor (c-kit ligand), granulocyte-macrophage colony stimulating factor and interleukin 3 on hematopoietic progenitors in human long-term bone marrow cultures. Stem Cells *11*, 435–444.

Lento, W., Congdon, K., Voermans, C., Kritzik, M., and Reya, T. (2013). Wnt signaling in normal and malignant hematopoiesis. Cold Spring Harb. Perspect. Biol. *5*, a008011.

Lis, R., Karrasch, C.C., Poulos, M.G., Kunar, B., Redmond, D., Duran, J.G.B., Badwe, C.R., Schachterle, W., Ginsberg, M., Xiang, J., et al. (2017). Conversion of adult endothelium to immunocompetent haematopoietic stem cells. Nature *545*, 439–445.

Luker, K.E., Pata, P., Shemiakina, I.I., Pereverzeva, A., Stacer, A.C., Shcherbo, D.S., Pletnev, V.Z., Skolnaja, M., Lukyanov, K.A., Luker, G.D., et al. (2015). Comparative study reveals better far-red fluorescent protein for whole body imaging. Sci. Rep. *5*, 10332.

Mikkola, H.K.A. (2006). The journey of developing hematopoietic stem cells. Development *133*, 3733–3744.

Morgan, R.A., Gray, D., Lomova, A., and Kohn, D.B. (2017). Hematopoietic stem cell gene therapy: progress and lessons learned. Cell Stem Cell *21*, 574–590.

Park, M.A., Kumar, A., Jung, H.S., Uenishi, G., Moskvin, O.V., Thomson, J.A., and Slukvin, I.I. (2018). Activation of the arterial program drives development of definitive hemogenic endothelium with lymphoid potential article activation of the arterial program drives development of definitive hemogenic endothelium with lymphoid potential. Cell Rep. *23*, 2467–2481.

Prokhorova, T.A., Harkness, L.M., Frandsen, U., Ditzel, N., Schrøder, H.D., Burns, J.S., and Kassem, M. (2009). Teratoma formation by human embryonic stem cells is site dependent and enhanced by the presence of Matrigel. Stem Cells Dev. *18*, 47–54.

Selich, A., Daudert, J., Hass, R., Philipp, F., von Kaisenberg, C., Paul, G., Cornils, K., Fehse, B., Rittinghausen, S., Schamnbach, A., et al. (2016). Massive clonal selection and transiently contributing clones during expansion of mesenchymal stem cell cultures revealed by Lentiviral RGB-Barcode technology. Stem Cells Transl. Med. *5*, 591–601.

Sugimura, R., Jha, D.K., Han, A., Soria-Valles, C., da Rocha, E.L., Lu, Y.-F., Goettel, J.A., Serrao, E., Rowe, R.G., Malleshaiah, M., et al. (2017). Haematopoietic stem and progenitor cells from human pluripotent stem cells. Nature *545*, 432–438.

Suzuki, N., Yamazaki, S., Yamaguchi, T., Okabe, M., Masaki, H., Takaki, S., Otsu, M., and Nakauchi, H. (2013). Generation of engraftable hematopoietic stem cells from induced pluripotent stem cells by way of teratoma formation. Mol. Ther. *21*, 1424–1431.

Tsukada, M., Ota, Y., Wilkinson, A.C., Becker, H.J., Osato, M., Nakauchi, H., and Yamazaki, S. (2017). In vivo generation of engraftable murine hematopoietic stem cells by Gfi1b, c-Fos, and Gata2 overexpression within teratoma. Stem Cell Reports *9*, 1024–1033.

Vo, L.T., and Daley, G.Q. (2015). De novo generation of HSCs from somatic and pluripotent stem cell sources. Blood *125*, 2641–2648.

Yamaguchi, H., Ishii, E., Saito, S., Tashiro, K., Fujita, I., Yoshidomi, S., Ohtubo, M., Akazawa, K., and Miyazaki, S. (1996). Umbilical vein endothelial cells are an important source of c-kit and stem cell factor which regulate the proliferation of haemopoietic progenitor cells. Br. J. Haematol. *94*, 606–611.

Yildirim, S., Boehmler, A.M., Kanz, L., and Möhle, R. (2005). Expansion of cord blood CD34+ hematopoietic progenitor cells in coculture with autologous umbilical vein endothelial cells (HUVEC) is superior to cytokine-supplemented liquid culture. Bone Marrow Transpl. *36*, 71–79.

Stem Cell Reports, Volume *11*

Supplemental Information

Human Teratoma-Derived Hematopoiesis Is a Highly Polyclonal Process Supported by Human Umbilical Vein Endothelial Cells

Friederike Philipp, Anton Selich, Michael Rothe, Dirk Hoffmann, Susanne Rittinghausen, Michael A. Morgan, Denise Klatt, Silke Glage, Stefan Lienenklaus, Vanessa Neuhaus, Katherina Sewald, Armin Braun, and Axel Schambach

Figure S1. Flow cytometric analysis of teratoma samples and generation of hematopoietic supporter cell types. Related to Figures 1 and 2 .

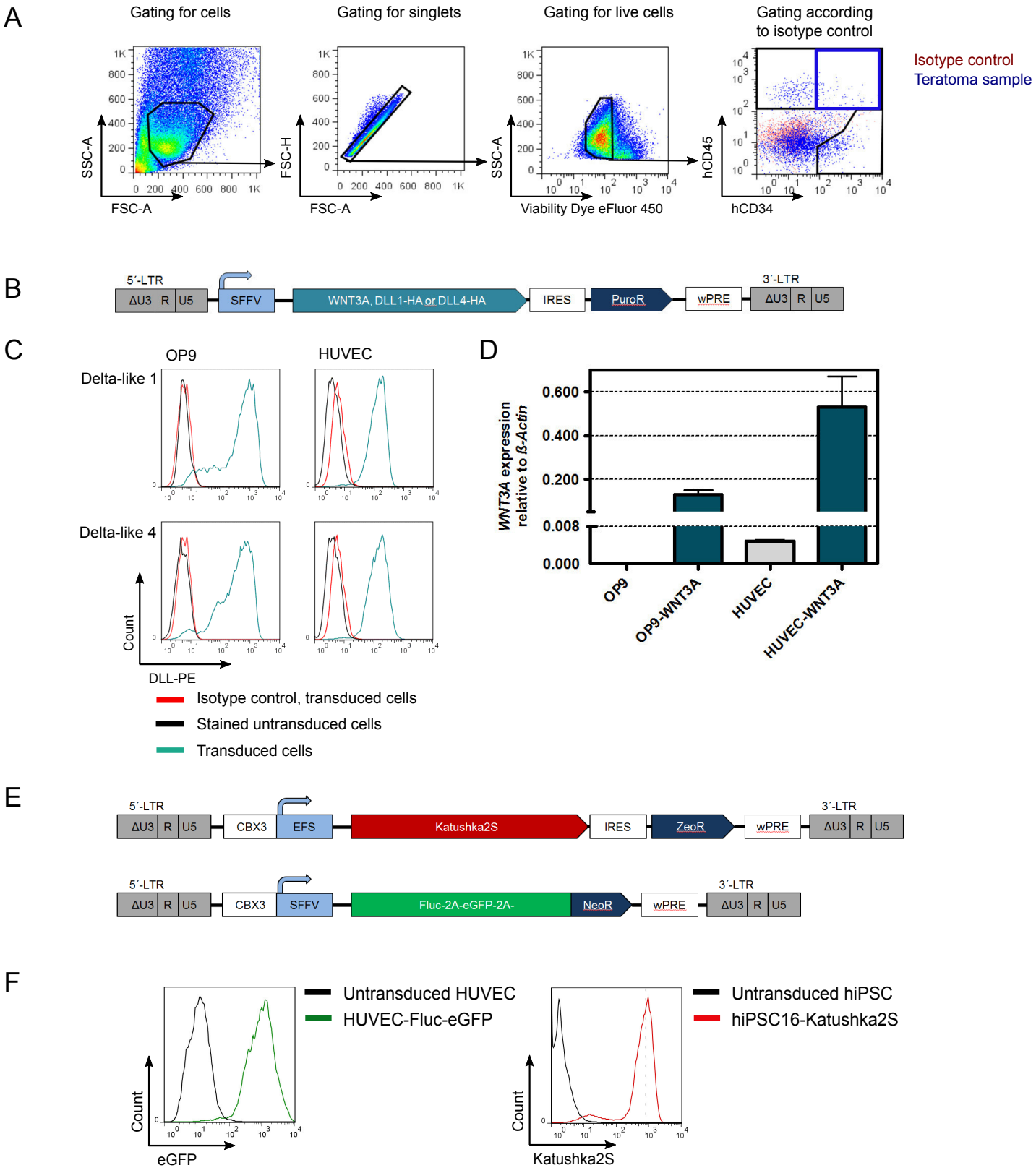

Figure S1. Flow cytometry (FC) analysis of teratoma samples and generation of hematopoietic supporter cell lines. Related to Figures 1 and 2. (A) Gating strategy for FC analysis of hematopoietic cells in teratoma samples. After cells were gated in SSC/FSC, doublets were excluded. Then, living cells were selected by viability staining. Gates were set according to isotype controls. (B) Lentiviral vector for the overexpression of DLL1, DLL4 and WNT3A in OP9 and HUVEC. (C) Notch ligand overexpression in transduced OP9 or HUVEC prior to co-injection for teratoma formation. Untransduced OP9 and HUVEC were stained as negative controls. (D) Quantitative PCR to determine *WNT3A* mRNA levels in HUVEC-WNT3A or OP9-WNT3A. *WNT3A* expression was related to *ß-Actin* mRNA level. Graph shows technical replicates n=3, mean and SD. (E) Lentiviral constructs for Katushka2S and firefly luciferase (Fluc) expression. (F) Expression analysis of transduced HUVEC-Fluc-eGFP and hiPSC-Kat by FC. Untransduced cells were used as controls.

Figure S2. Identification of hematopoietic, endothelial and mesenchymal cells by immunohistochemistry. Related to Figure 3.

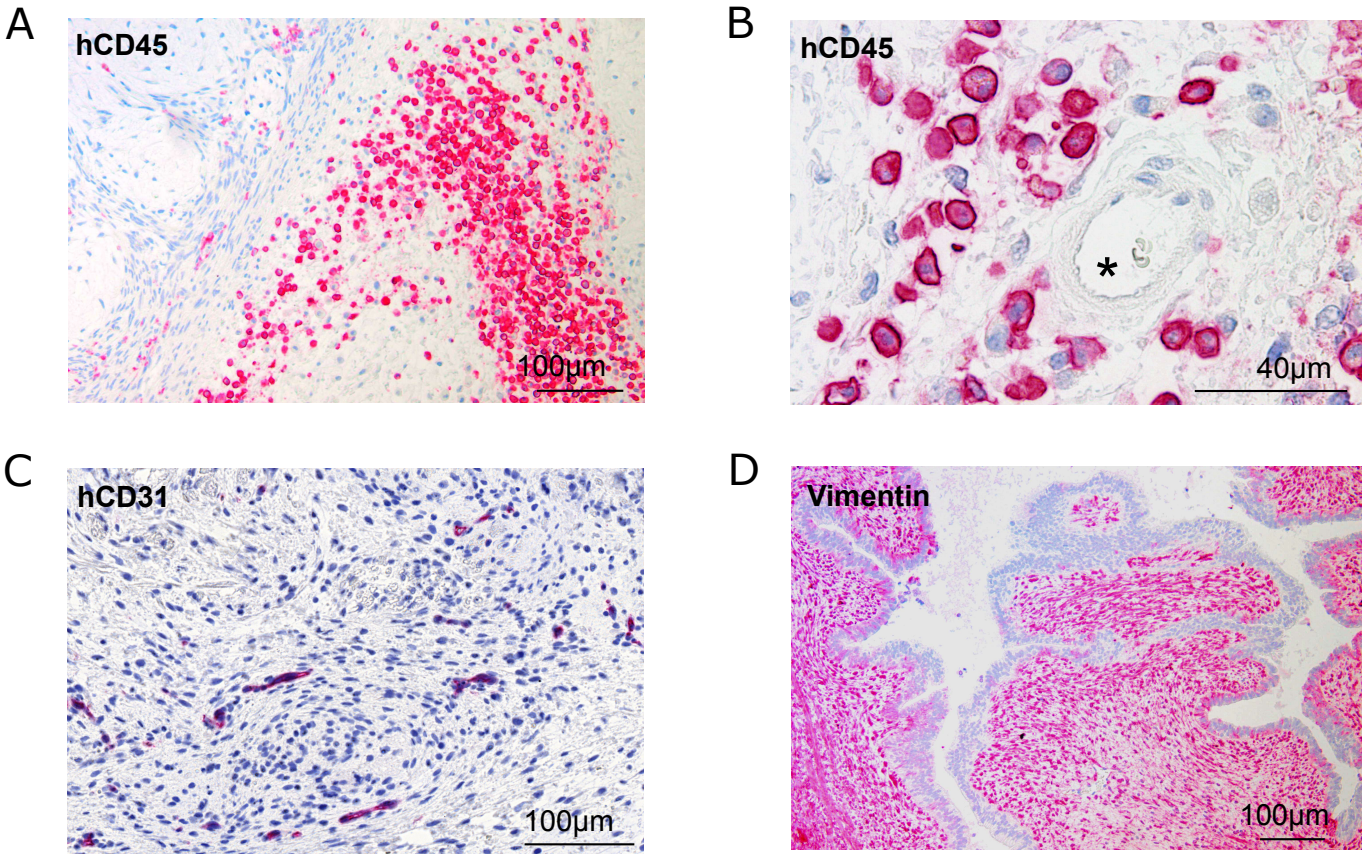

Figure S2. Identification of hematopoietic, endothelial and mesenchymal cells by chromogen immunohistochemistry (IHC) on hiPSC-derived teratomas generated in NSGS mice. Related to Figure 3. (A) Staining of human hematopoietic marker CD45. (B) Hematopoietic cells (CD45) in teratoma tissue close to a blood vessel which is labeled with *. (C) Human endothelial cells, marked by CD31. (D) Staining of mesenchymal marker Vimentin.

Supplemental experimental procedures

Cell culture

Human iPSC were co-cultured on murine embryonic fibroblasts C3H (kindly provided by T. Cantz, Hannover Medical School) according to standard protocols. Unless stated otherwise, the iPSC clone CD34iPSC16 was used (Lachmann *et al*., 2014). hiPSC cultures were maintained in Knockout DMEM (Gibco) supplemented with 20 % KO serum replacement (Gibco), 1 % NEAA (Gibco), 2 mM glutamine (Biochrom), 0.1 mM β-mercaptoethanol (Sigma-Aldrich), 100 U/ml penicillin and 100 µg/ml streptomycin (PAA) and 20 ng/ml bFGF (kindly provided by the Department of Technical Chemistry, Leibniz University Hannover). OP9 and HUVEC (VeraVec, Angiocrine Bioscience) were cultivated on 0.1 % gelatin coated flasks. Detachment was done with Trypsin/EDTA (Pan Biotech). OP9 cells were cultured in αMEM Medium +GlutaMAX-I (Gibco) supplemented with 100 U/ml penicillin and 100 µg/ml streptomycin (PAA) and 15 % fetal bovine serum (Brazil One, Pan Biotech). HUVEC were cultured in Medium199 (Gibco), 20 U/ml Heparin (Ratiopharm), 10 mM HEPES buffer (PAA), 2 mM glutamine (Merck), 100 U/ml penicillin, 100 µg/ml streptomycin (PAA) and 20-40 µg/ml endothelial cell growth supplement (Sigma-Aldrich).

Lentiviral constructs

Lentiviral vectors for Notch ligands and WNT3A expression were constructed by using a 3rd generation lentiviral vector (kindly provided by L. Naldini, Instituto Scientifico San Raffaele, Italy) equipped with the SFFV U3 promoter (Schambach et al., 2006) by inserting the human DLL1, DLL4 and WNT3A cDNAs amplified via PCR as AgeI and SalI fragments. A 3' HA-tag was included for both DLL fragments. Thereafter, an IRES.Puromycin resistance cassette was introduced as a SalI and XhoI fragment into the vector. Final vectors pRRL.PPT.SFFV.DLL1-HA.IRES.PuroR.pre, pRRL.PPT.SFFV.DLL4-HA.IRES.PuroR.pre and pRRL.PPT.SFFV.WNT3A.IRES.PuroR.pre were used for viral supernatant production. The design and generation of barcoded vectors has been described before (Cornils et al., 2014). The vector was modified by exchanging the spleen focus forming virus promoter with elongation factor 1α, short CBX3 element (CBX3.EFS), to prevent gene silencing (Hoffmann et al., 2017; Müller-Kuller et al., 2015). The lentiviral vector for firefly luciferase (Fluc) expression, combined with Neomycin resistant gene and eGFP, was cloned as a three fragment ligation after PCR amplification of FLuc.T2A.eGFP (kindly provided by S. Waddington) (Buckley et al., 2015) as BamHI and XbaI fragment and P2A.Neomycin as XbaI and SalI fragment into the lentiviral pRRL backbone with CBX3 element (pRRL.PPT.CBX3.SFFV.FLuc.2A.eGFP.2A.NeoR.pre). For Katushka2S expression (Luker et al., 2015), the Katushka2S nucleotide sequence was synthesized by GeneArt (Thermo Fisher Scientific) as a fragment flanked by BamHI and MluI restriction sites. The Katushka2S fragment and an IRES.Zeocin resistance cassette as MluI and SalI fragment were cloned into the lentiviral pRRL vector containing the CBX3.EFS promoter (pRRL.PPT.CBX3.EFS.Katushka.IRES.ZeoR.pre). Further cloning details are available on request.

Virus production

Virus production was performed with a lentiviral four-plasmid split packaging system and calcium precipitation as described before (Maetzig et al., 2014), using vector as well as gag/pol, envelope and VSVg helper plasmids. For the barcode constructs, virus titrations were performed as described elsewhere (Kraunus et al., 2004). Briefly, HT1080 cells were transduced and cultured until isolation of genomic DNA with QIAampDNABlood Mini Kit (Qiagen). Vector copy number (VCN) was determined by multiplex qPCR on viral woodchuck hepatitis virus post regulatory element and genomic PTBP2 (Rothe et al., 2012). Quantitative PCRs were performed on the ABI StepOne Plus (Applied Biosystems).

Transductions

All lentiviral transductions were performed in the presence of 4 µg/ml protamine sulfate (Maetzig et al., 2014). For transduction of hiPSCs with barcode constructs, cultures were treated with 10 µM Y-27632 one hour before harvest with Trypsin/EDTA (PAA). Cells were incubated together with the respective amount of virus supernatant (MOI= 1.5) for one hour at 37°C. Cells remained resuspended by tipping the tube every 15 minutes. Afterwards, cells were seeded onto wells coated with 0.25 % Geltrex (Thermo Fisher Scientific). Medium change was performed after 6-12 hours and contained 10 µM Y-27632. Transduced cells were sorted by FACS by means of fluorescent protein expression and kept as monolayers. Conditioned medium for monolayers was prepared by incubating hiPSC medium for 24 hours on C3H cultures followed by filtration through a 0.22 µm syringe filter (Millipore). For transduction of HUVEC and OP9, cells were plated with 30 % confluency on 6 well plates one day before transduction. The next day, medium was replaced by viral supernatant and incubated for 4-6 hours followed by a medium change. Transduced cells were selected by puromycin (Invivogen, OP9 7 µg/ml, HUVEC 3 µg/ ml) or neomycin (HUVEC 500 µg/ml). Katushka2S expressing hiPSC colonies were picked and checked for transgene expression by flow

cytometry. Nucleotide barcode labeled hiPSC were sorted for fluorescent reporter expression. Vector copy numbers were determined as described for virus transduction earlier.

qPCR to determine *WNT3A* expression
Cell cultures were harvested and RNA was isolated with RNeasy Mini Kit (Qiagen) according to manufacturer's protocol. RNA (600 ng) was transcribed to cDNA using QuantiTect Reverse Transcription Kit (Qiagen). Quantitative PCR was accomplished with SYBR Green (Qiagen) and a StepOnePlus Real-Time PCR System (Thermo Fisher Scientific). Primer for *WNT3A*, murine and human β-*Actin* amplification were described before (Galla et al., 2011, 2013; Mazzotta et al., 2016). 58°C was used as annealing temperature. Expression differences were calculated by ΔΔCt method (Pfaffl, 2001). Initial murine *Wnt3a* level in OP9 was not determined.

Mice
NSG (NOD.Cg-Prkdcscid Il2rgtm1Wjl/SzJ) and NSGS (NOD.Cg-Prkdcscid Il2rgtm1Wjl Tg(CMV-IL3,CSF2,KITLG)1Eav/MloySzJ) mice were kept in pathogen-free environment with access to food and water at the animal facility of Hannover Medical School. Females between 7 and 21 weeks were used for teratoma assays. Both strains were bred at Hannover Medical School according to animal protection laws.

Flow cytometry (FC)
Teratoma cells were incubated with Fixable Viability Dye eFluor™ 450 (Thermo Fisher Scientific) and human and murine Fc block TruStainFcX for 30 minutes on ice in the dark (#101320, #422302, Biolegend). Antibodies and corresponding isotype controls are listed below. Data was acquired with LSRII or FACSCalibur (both BD Bioscience). Data analyses were performed with FlowJo software (TriStar). Viability staining was not used for FC of cell cultures. All other staining and FC protocols were as described above.

Antibodies used for flow cytometry analysis:

Antibody for flow cytometry	Catalog number	Manufacturer	Isotype
anti-human CD34-APC	343510	Biolegend	Mouse IgG1, κ
anti-human CD34-PE/Cy7	343516	Biolegend	Mouse IgG1, κ
anti-human CD45-BV570	304033	Biolegend	Mouse IgG1, κ
anti-human CD45-FITC	304006	Biolegend	Mouse IgG1, κ
anti-human CD43-PE	12-0439-42	eBioscience	Mouse IgG1
anti-human CD31-PE	130-092-653	Miltenyi	Mouse IgG1, κ
anti-human DLL1-PE	346403	Biolegend	Mouse IgG1, κ
anti-human DLL4-PE	346505	Biolegend	Mouse IgG1, κ
Isotypes			
Mouse IgG1-APC	400120	Biolegend	
Mouse IgG1 -PE/Cy7	400126	Biolegend	
Mouse IgG1-BV570	400159	Biolegend	
Mouse IgG1-FITC	400110	Biolegend	
Mouse IgG1-PE	400112	Biolegend	

Longitudinal study
NSGS mice of 7-13 weeks were anesthetized with 2-3 % isofluorane (CP Pharma) and the lower back was shaved with an electric shaver. Teratoma inductions were carried out as described above. Luciferin (Intrace Medial SA) application was done by injection by tail vein injection (150 µg/ g, 100 µl/ 20 g in PBS). Images were captured approximately 10 minutes after luciferin injection using an IVIS SpectrumCT and software Living Image 4.5.5 (both PerkinElmer). Katushka2S was imaged with a 605/660 nm filter set.

Clonogenic assays
Teratoma cells were sorted with BD FACSARIA Fusion and software BD FACSDIVA (both BD Bioscience) for $CD34^+/CD45^+$ cells, following the gating strategy of FC analysis. Freshly isolated $CD34^+$ cord blood (CB) cells were used as positive control. CB was obtained after written consent. Mononuclear cells were separated with a densitiy gradient using Biocoll Separating Solution (Biochrom) and 50 ml LeucoSEP tubes (Fisher Scientific) according to the manufacturer's protocol. Isolation of $CD34^+$ cells was done with CD34 MicroBead Kit (Miltenyi, 13046702). Cells were counted and up to 2500 teratoma cells and up to 2000 CB cells were seeded in 1.5 ml Methocult Optimum 4034 (STEMCELL Technologies) with 100 U/ml penicillin and 100 µg/ml streptomycin (PAA) (Corning).

Colonies were scored after 14 days of incubation. Colonies of the same CFU type were then picked and pooled for cytospins.

Cytospin and analysis
Cells were centrifuged in 150 µl for 10 minutes at 450 rpm by a ThermoShandon Cytospin 4 cytocentrifuge (Thermo Fisher Scientific). Staining was performed according to the Pappenheim protocol. For that, slides were incubated in May-Gruenwald staining solution (Carl Roth) for 5 minutes. Afterwards, slides were washed in PBS and left in Giemsa solution (Sigma-Aldrich) for 15 minutes. Samples were mounted using Roti®Histokitt (CarlRoth). Pictures were taken with a BX51 microscope, camera XC50 and software Cell^F version 3.4 (all Olympus).

Immunohistochemistry (IHC)
Isolated tissue was fixed overnight at room temperature in 4 % neutral buffered formaldehyde (Carl Roth). Then, samples were embedded in paraffin and sliced in 3 µm sections. After deparaffinization, antigen retrieval was achieved by heat and citrate buffer. All antibodies and dilutions are listed below. Prior to staining, specimens were blocked using donkey (Jackson ImmunoResearch Inc) or goat serum (Vector Laboratories Inc). Incubations with primary antibody were conducted overnight at 4°C. In case of fluorescent staining, secondary antibodies were incubated for four to six hours at room temperature. Nuclei were stained with TO-PRO-3 Iodide (Thermo Fisher Scientific). Samples were mounted with Immunoselect Antifading mounting medium (Dianova). For 3D imaging of vasculature in teratoma, tissue was fixed in 2 % formaldehyde/ PBS overnight at 4°C, embedded in 2 % agarose blocks and sliced in 200 µm slices with a vibratom (Campden Instruments). During staining procedure, slices were kept in 300 µl PBS solution in 12 well plates. The same dilutions of antibodies were used as for IHC described above, but incubation times were increased to overnight for blocking and to 24 hours for antibodies at 4°C. Mounting was done with ProLong™ Gold Antifade Reagent (Thermo Fisher Scientific). Pictures were taken with Confocal LSM Meta 512 and ZEN 2009 and processed with software AxioVision SE64Rel.4.9 (all Zeiss) and Imaris Version 7.6.5 (Bitplane AG). For chromogen IHC, we applied a routine method using the Dako REAL™ Detection System and Alkaline Phosphatase/RED (Dako) staining kit. The slides were finally counterstained with Mayer's hematoxylin (Merck) and mounted with xylol (CG Chemikalien) or Eukitt (Sigma-Aldrich). Pictures were taken with a BX51 microscope outfitted with an XC50 camera and Cell^F version 3.4 software (all Olympus).

Antibodies and dilutions used for immunohistochemistry (IHC) on paraffin-embedded tissue:

1st antibody for IHC	Catalog number	Manufacturer	Applied dilution
anti-human CD34	AF7227	RD Systems	1:50
anti-human CD45	M0701	Dako	1:100
anti-human CD31	ab76533	Abcam	1:100
anti-human vimentin V9	M0725	Dako	1:100
anti-human CD43	NBP2-33746	Novus	1:80
Isotypes			
Sheep-IgG, polyclonal	5-001-A	RD Systems	According to 1st antibody
Rabbit-IgG, monoclonal	ab172730	Abcam	According to 1st antibody
Mouse-IgG1 κ, monoclonal	X0931	Dako	According to 1st antibody
2nd antibody for fluorescent IHC			
Donkey-anti-sheep-IgG-AlexaFluor488 (H+L)	713-546-147	Jackson ImmunoResearch Inc	1:800
Donkey-anti-mouse-IgG-AlexaFluor647(H+L)	715-605-150	Jackson ImmunoResearch Inc	1:400
Donkey-anti-rabbit-IgG-Cy3 (H+L)	711-165-152	Jackson ImmunoResearch Inc	1:400
2nd antibody for chromogen IHC	Catalog number	Manufacturer	Applied dilution
Donkey-anti-sheep-IgG-Biotin (H+L)	713-065-147	Jackson ImmunoResearch Inc	1:1000
Goat-anti-mouse-IgG-Biotin (H+L)	115-065-166	Jackson ImmunoResearch Inc	1:800

High throughput sequencing of genetic barcodes

Barcodes were analyzed by deep sequencing as described before (Selich *et al*., 2016). In short, barcodes were amplified by a nested PCR and PCR mixMyFi Mix 23 (Bioline). Individual samples were then labeled by next generation sequencing with adapter-containing index primers. Pooled samples were sequenced by IonTorrent ™ PGM method (Thermo Fisher Scientific). Sequences were then assigned to the samples by a custom Perl 5 script (https://www.perl.org). To remove unspecific amplicons, the sequences were screened for the conserved nucleotides "TACCATCTAGA" and "CTCGAGACT" flanking the barcode region. The last steps of data analysis were performed with customized R scripts (https://www.R-project.org). The histogram was visualized with the R package ggplot2 (Wickham, 2009). Venn diagrams were made with the R package VennDiagram (Chen and Boutros, 2011). Further details are available on request.

Supplemental references

Buckley, S.M.K., Delhove, J.M.K.M., Perocheau, D.P., Karda, R., Rahim, A.A., Howe, S.J., Ward, N.J., Birrell, M.A., Belvisi, M.G., Arbuthnot, P., et al. (2015). In vivo bioimaging with tissue-specific transcription factor activated luciferase reporters. Sci. Rep. *5*, 11842.

Chen, H., and Boutros, P.C. (2011). VennDiagram: a package for the generation of highly-customizable Venn and Euler diagrams in R. BMC Bioinformatics *12*, 35.

Galla, M., Schambach, A., Falk, C.S., Maetzig, T., Kuehle, J., Lange, K., Zychlinski, D., Heinz, N., Brugman, M.H., Göhring, G., et al. (2011). Avoiding cytotoxicity of transposases by dose-controlled mRNA delivery. Nucleic Acids Res. *39*, 7147–7160.

Galla, M., Schambach, A., and Baum, C. (2013). Retrovirus-based mRNA transfer for transient cell manipulation. Methods Mol. Biol. *969*, 139–161.

Hoffmann, D., Schott, J.W., Geis, F.K., Lange, L., Müller, F.J., Lenz, D., Zychlinski, D., Steinemann, D., Morgan, M., Moritz, T., et al. (2017). Detailed comparison of retroviral vectors and promoter configurations for stable and high transgene expression in human induced pluripotent stem cells. Gene Ther. *24*, 298–307.

Kraunus, J., Schaumann, D.H.S., Meyer, J., Modlich, U., Fehse, B., Brandenburg, G., von Laer, D., Klump, H., Schambach, A., Bohne, J., et al. (2004). Self-inactivating retroviral vectors with improved RNA processing. Gene Ther. *11*, 1568–1578.

Lachmann, N., Happle, C., Ackermann, M., Lüttge, D., Wetzke, M., Merkert, S., Hetzel, M., Kensah, G., Jara-Avaca, M., Mucci, A., et al. (2014). Gene correction of human induced pluripotent stem cells repairs the cellular phenotype in pulmonary alveolar proteinosis. Am. J. Respir. Crit. Care Med. *189*, 167–182.

Maetzig, T., Kuehle, J., Schwarzer, A., Turan, S., Rothe, M., Chaturvedi, A., Morgan, M., Ha, T.C., Heuser, M., Hammerschmidt, W., et al. (2014). All-in-One inducible lentiviral vector systems based on drug controlled FLP recombinase. Biomaterials *35*, 4345–4356.

Mazzotta, S., Neves, C., Bonner, R.J., Bernardo, A.S., Docherty, K., and Hoppler, S. (2016). Distinctive Roles of Canonical and Noncanonical Wnt Signaling in Human Embryonic Cardiomyocyte Development. Stem Cell Reports *7*, 764–776.

Müller-Kuller, U., Ackermann, M., Kolodziej, S., Brendel, C., Fritsch, J., Lachmann, N., Kunkel, H., Lausen, J., Schambach, A., Moritz, T., et al. (2015). A minimal ubiquitous chromatin opening element (UCOE) effectively prevents silencing of juxtaposed heterologous promoters by epigenetic remodeling in multipotent and pluripotent stem cells. Nucleic Acids Res. *43*, 1577–1592.

Pfaffl, M.W. (2001). A new mathematical model for relative quantification in real-time RT-PCR. Nucleic Acids Res. *29*, 45e–45.

Rothe, M., Rittelmeyer, I., Iken, M., Rüdrich, U., Schambach, A., Glage, S., Manns, M.P., Baum, C., Bock, M., Ott, M., et al. (2012). Epidermal growth factor improves lentivirus vector gene transfer into primary mouse hepatocytes. Gene Ther. *19*, 425–434.

Schambach, A., Bohne, J., Chandra, S., Will, E., Margison, G.P., Williams, D.A., and Baum, C. (2006). Equal potency of gammaretroviral and lentiviral SIN vectors for expression of O6-methylguanine–DNA methyltransferase in hematopoietic cells. Mol. Ther. *13*, 391–400.

Wickham, H. (2009). ggplot2 (New York, NY: Springer New York).